TABLES OF ANTENNA CHARACTERISTICS

TABLES OF ANTENNA CHARACTERISTICS

Ronold W. P. King

Gordon McKay Professor of Applied Physics
Harvard University
Cambridge, Massachusetts

IFI/PLENUM • NEW YORK–WASHINGTON–LONDON • 1971

Library of Congress Catalog Card Number 74-157425

SBN 306-65154-8

A Subsidiary of Plenum Publishing Corporation
227 West 17th Street, New York, N.Y. 10011

United Kingdom edition published by Plenum Press, London
A Division of Plenum Publishing Company, Ltd.
Davis House (4th Floor), 8 Scrubs Lane, Harlesden, NW 10 6SE, England

Printed in the United States of America

Preface

Important practical properties of antennas are their driving-point admittances and far-field patterns. The accurate determination of these and other related characteristics requires the explicit or implicit solution of integral equations for the current distributions along the radiating structure. This can be accomplished with the help of analytical and numerical techniques; the validity of approximations can be checked experimentally.

In order to obtain specific data for practical applications, high-speed computers may be used to evaluate analytically derived formulas or, where these are unavailable, to obtain direct numerical solutions. Programs written for such a purpose are usually long and complicated, and they may require very fast machines with large storage capacity. Since these are not generally available outside of large organizations, a representative set of numerical tables to provide a variety of useful characteristics of cylindrical and loop antennas and dipole arrays should be of value.

Over a period of years extensive researches on antennas have been carried out at Harvard University with the support of the U.S. Navy, the U.S. Air Force, and the Signal Corps of the U.S. Army under Contracts N00014-67-A-0298-0005 and F19(628)-C-0030. A selection from the results of these investigations has been prepared, recomputed, and tabulated for this book. The researches include contributions by D. C. Chang, V. W. H. Chang, C. W. Harrison, Jr., S. S. Sandler, C. Y. Ting, and T. T. Wu. The programming was carried out primarily by Barbara Sandler and Georgia Efthymiopoulou, but important contributions were also made by E. A. Aronson at the Sandia Corporation, Margaret Owens, and Irma Rivera-Veve. The typing, checking, and proofreading were done by Margaret Owens. The figures were prepared with the assistance of Elmer Rising and his staff; photographic work was carried out by Armand Dionne.

Cambridge, Massachusetts
July 1970

RONOLD W. P. KING

Contents

1. The Complex Wave Number k and the Normalizing Factor Δ

The characteristics of antennas described and tabulated in this volume are obtained from solutions of Maxwell's equations in an infinite, homogeneous, isotropic medium characterized by the complex permittivity $\varepsilon = \varepsilon_0\varepsilon_r = \varepsilon_0(\varepsilon_r'' - j\varepsilon_r')$, the complex conductivity $\sigma = \sigma' - j\sigma''$, and the real permeability $\mu = \mu_0\mu_r$. In such a medium Maxwell's equations have the form

$$\nabla \times E = -j\omega B, \qquad \nabla \cdot E = 0 \tag{1.1}$$

$$\nabla \times B = \mu(\sigma + j\omega\varepsilon)E, \qquad \nabla \cdot B = 0 \tag{1.2}$$

In air $\sigma = 0$, $\varepsilon = \varepsilon_0$, $\mu = \mu_0$. The complex quantity $\sigma + j\omega\varepsilon$ can be separated into its real and imaginary parts such that

$$\sigma + j\omega\varepsilon = \sigma_e + j\omega\varepsilon_e \tag{1.3}$$

where the real effective conductivity σ_e and the real effective permittivity ε_e are given by

$$\sigma_e = \sigma' + \omega\varepsilon_0\varepsilon_r'', \qquad \varepsilon_e = \varepsilon_0\left(\varepsilon' - \frac{\sigma''}{\omega\varepsilon_0}\right) = \varepsilon_0\varepsilon_{er} \tag{1.4}$$

When the variables in Maxwell's equations are separated, these yield the second-order vector wave equation

$$\nabla^2 E + k^2 E = 0 \tag{1.5}$$

and a similar equation for B. The complex wave number or propagation constant k is related to $(\sigma_e + j\omega\varepsilon_e)$ by

$$k^2 = \omega^2\mu\varepsilon_e(1 - jp_e) = \omega^2\mu\varepsilon_e - j\omega\mu\sigma_e \tag{1.6}$$

where

$$p_e = \frac{\sigma_e}{\omega\varepsilon_e} = \frac{\sigma_e}{\omega\varepsilon_0\varepsilon_{er}} \tag{1.7}$$

is the loss tangent. The explicit formulas for the real and imaginary parts β and α of $k = \beta - j\alpha$ are obtained as follows:

$$\varepsilon_e > 0: \qquad k = \omega\sqrt{\mu\varepsilon_e}\sqrt{1 - jp_e}$$

$$= k_0\sqrt{\mu_r\varepsilon_{er}}[f(p_e) - jg(p_e)] \tag{1.8a}$$

$$\varepsilon_e = 0: \qquad k = \sqrt{j\omega\mu\sigma_e} = \sqrt{\frac{\omega\mu\sigma_e}{2}}(1 - j)$$

$$= k_0\sqrt{\frac{\mu_r\sigma_e}{2\omega\varepsilon_0}}(1 - j) \tag{1.8b}$$

$$\varepsilon_e < 0: \qquad k = -j\omega\sqrt{\mu|\varepsilon_e|}\sqrt{1 + j|p_e|}$$

$$= k_0\sqrt{\mu_r|\varepsilon_{er}|}[g(|p_e|) - jf(|p_e|)] \tag{1.8c}$$

where

$$k_0 = \omega\sqrt{\mu_0\varepsilon_0}, \qquad \mu_0 = 4\pi \times 10^{-7} \text{ henries/m}, \qquad \varepsilon_0 = 8.854 \times 10^{-12} \text{ farads/m} \tag{1.9}$$

The functions $f(p)$ and $g(p)$ are defined by

$$f(p) = \cosh(\tfrac{1}{2}\sinh^{-1} p) = \sqrt{\tfrac{1}{2}(\sqrt{1 + p^2} + 1)} \tag{1.10a}$$

$$g(p) = \sinh(\tfrac{1}{2}\sinh^{-1} p) = \sqrt{\tfrac{1}{2}(\sqrt{1 + p^2} - 1)} \tag{1.10b}$$

It follows that with $\zeta_0 = \sqrt{\mu_0/\varepsilon_0} \doteq 120\pi$ ohms,

$$\varepsilon_{er} > 0: \qquad \beta = k_0\sqrt{\mu_r\varepsilon_{er}}\,f(p_e) = \frac{\sigma_e\zeta_0}{\sqrt{\varepsilon_{er}}}\frac{f(p_e)}{p_e} \tag{1.11a}$$

$$\alpha = k_0\sqrt{\mu_r\varepsilon_{er}}\,g(p_e) = \frac{\sigma_e\zeta_0}{\sqrt{\varepsilon_{er}}}\frac{g(p_e)}{p_e} < \beta \tag{1.11b}$$

$$\varepsilon_{er} = 0: \qquad \beta = \alpha = \sqrt{\frac{\omega\mu\sigma_e}{2}} \tag{1.12}$$

$$\varepsilon_{er} < 0: \qquad \beta = k_0\sqrt{\mu_r|\varepsilon_{er}|}\,g(|p_e|) = \frac{\sigma_e\zeta_0}{\sqrt{|\varepsilon_{er}|}}\frac{g(|p_e|)}{|p_e|} \tag{1.13a}$$

$$\alpha = k_0\sqrt{\mu_r|\varepsilon_{er}|}\,f(|p_e|) = \frac{\sigma_e\zeta_0}{\sqrt{|\varepsilon_{er}|}}\frac{f(|p_e|)}{|p_e|} > \beta \tag{1.13b}$$

In addition to the propagation constant k, the complex wave impedance

$$\zeta = \frac{\omega\mu}{k} = \frac{\omega\mu}{\beta(1 - j\alpha/\beta)} = \frac{\zeta_0}{(1 - j\alpha/\beta)}\frac{\omega\mu}{\beta\zeta_0} \tag{1.14a}$$

where

$$\zeta_0 = \sqrt{\mu_0/\varepsilon_0} = 376.7 \text{ ohms} \doteq 120\pi \text{ ohms} \tag{1.14b}$$

frequently occurs as a multiplier in amplitudes. It is convenient to use the quantity

$$\Delta = \frac{\beta\zeta_0}{\omega\mu} = \frac{\beta}{k_0\mu_r} \tag{1.15}$$

as a general normalizing factor. Then

$$\zeta = \frac{\zeta_0}{\Delta(1 - j\alpha/\beta)} \tag{1.16}$$

where

$$\varepsilon_e > 0: \qquad \Delta = \sqrt{\varepsilon_{er}/\mu_r}\,f(p_e) \tag{1.17}$$

$$\varepsilon_e = 0: \qquad \Delta = \sqrt{\sigma_e/2\omega\varepsilon_0\mu_r} \tag{1.18}$$

$$\varepsilon_e < 0: \qquad \Delta = \sqrt{|\varepsilon_{er}|/\mu_r}\,g(|p_e|) \tag{1.19}$$

Note that as $\varepsilon_e \to 0$, $p_e \to \infty$, $f(|p_e|) \to g(|p_e|) \to \sqrt{|p_e|/2} = \sqrt{\sigma_e/2\omega\varepsilon_0|\varepsilon_{er}|}$. Thus, the value of Δ at $\varepsilon_e = 0$ is the limit as $|p_e| \to \infty$ of the values for $\varepsilon_e > 0$ and $\varepsilon_e < 0$. Clearly, when σ_e, ε_e, and μ are specified for any given medium, k and Δ can be determined from (1.11)–(1.13) and (1.17)–(1.19), respectively. For this purpose tables of $f(p)$ and $g(p)$ as defined in (1.10a,b) are convenient. The frequency dependence of α and β for any assigned set of values σ_e, ε_e, and μ is contained in $f(p)/p$ or $g(p)/p$ as seen from (1.11a,b) and (1.13a,b). The functions $f(p)$, $g(p)$, $f(p)/p$, and $g(p)/p$ are given in Table 1.1, in which p is the variable ranging from zero to large values. The following high- and low-frequency ranges and approximate formulas are useful:

$$0 \le p^2 \le 0.04: \qquad f(p) \doteq 1, \qquad g(p) \doteq p/2 \tag{1.20}$$

$$p^2 \ge 25: \qquad f(p) \doteq g(p) \doteq \sqrt{p/2} \tag{1.21}$$

For convenience in visualizing the behavior of these functions, graphs of $f(p)$, $g(p)$, $f(p)/p$, and $g(p)/p$ as functions of p are given in Fig. 1.1. Low- and high-frequency ranges are indicated, and frequency scales for dry earth ($\sigma_e = 10^{-3}$ mho/m, $\varepsilon_{er} = 7$), moist earth ($\sigma_e = 1.2 \times 10^{-2}$ mho/m, $\varepsilon_{er} = 15$), and wet earth ($\sigma_e = 3 \times 10^{-2}$ mho/m, $\varepsilon_{er} = 30$) are given. In Fig. 1.2, $f(p)/p$ and $g(p)/p$ are shown as functions of the frequency for these three types of earth. In ordinary dielectrics $\varepsilon_{er} \ge 1$ so that (1.11a,b) apply.

The properties of certain types of plasma over limited ranges of the parameters can be approximated by introducing real effective permittivities and conductivities given by

$$\varepsilon_{er} = 1 - \frac{Ne^2}{\varepsilon_0 m(\nu^2 + \omega^2)} = 1 - \frac{\omega_p^2}{\nu^2 + \omega^2} \tag{1.22}$$

$$\sigma_e = \frac{Ne^2\nu}{m(\nu^2 + \omega^2)} \tag{1.23}$$

where N is the number of electrons per unit volume; e is the charge and m the mass of the electron; ν is the collision frequency; and $\omega_p = 2\pi f_p$, where f_p is the plasma frequency. Note that when $\omega_p^2 < (\nu^2 + \omega^2)$, $0 < \varepsilon_{er} \le 1$, so that (1.11a,b) apply; when $\omega_p^2 = \nu^2 + \omega^2$, $\varepsilon_{er} = 0$, so that (1.12) applies; and when $\omega_p^2 > (\nu^2 + \omega^2)$, $\varepsilon_{er} < 0$, so that (1.13a,b) apply.

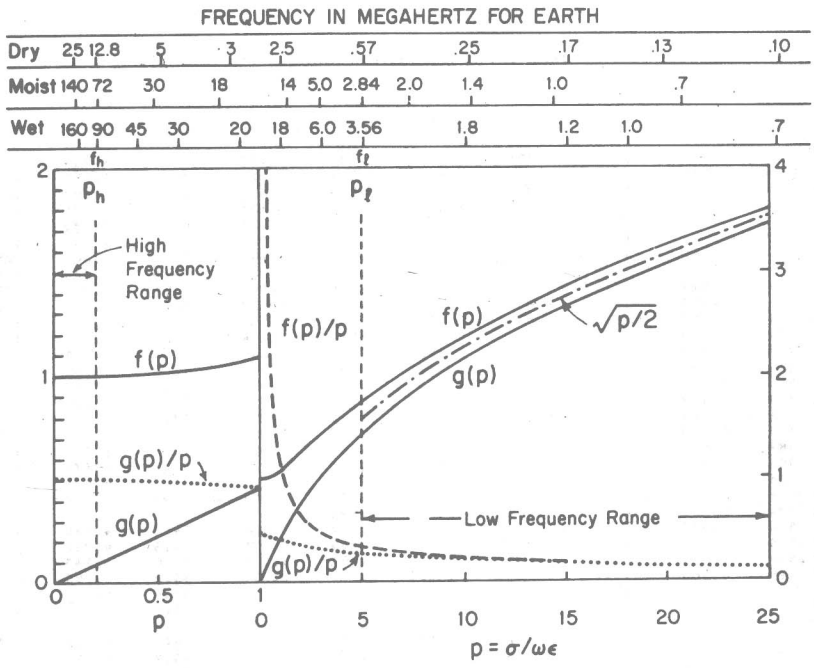

Fig. 1.1. The functions $f(p)$ and $g(p)$ and related quantities.

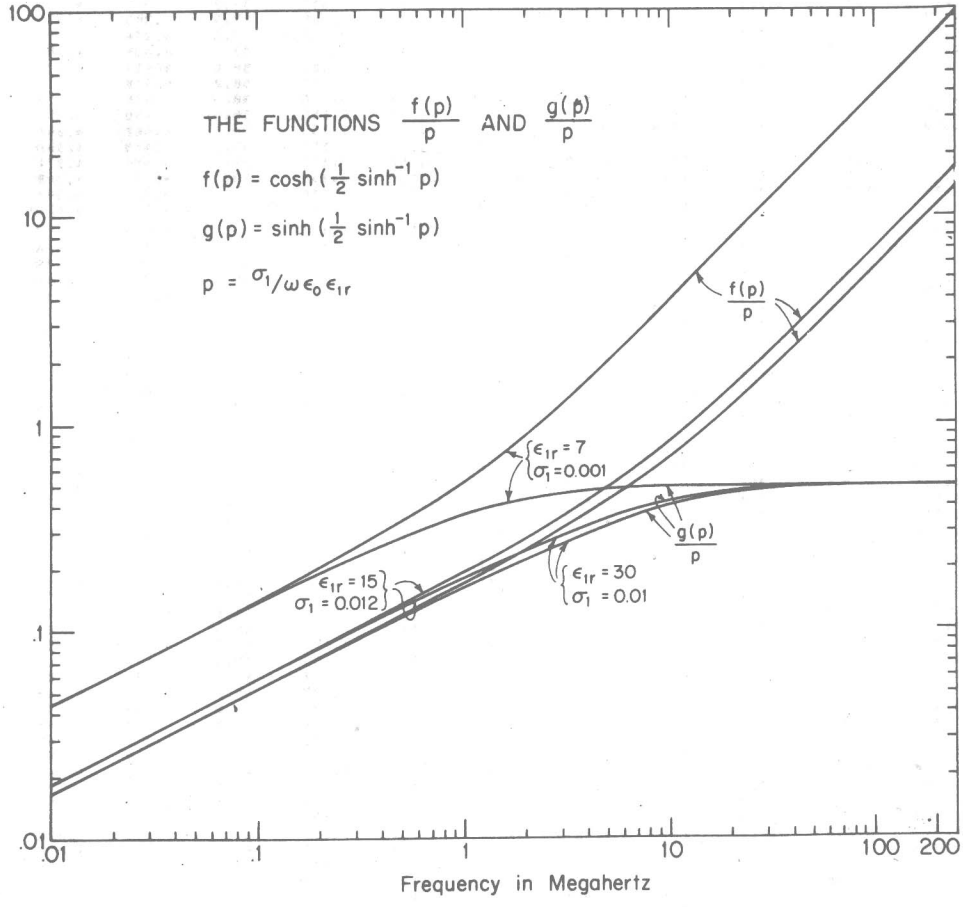

Fig. 1.2. The functions $f(p)/p$ and $g(p)/p$.

TABLE 1.1

TABLE OF F(P) AND G(P) FUNCTIONS

P	F(P)	G(P)	F(P)/P	G(P)/P	P	F(P)	G(P)	F(P)/P	G(P)/P	P	F(P)	G(P)	F(P)/P	G(P)/P
0.0	1.000	0.000	INF	0.500	10.0	2.351	2.127	0.235	0.213	30.0	3.938	3.809	0.131	0.127
0.1	1.001	0.050	10.012	0.499	10.2	2.372	2.153	0.233	0.211	30.2	3.951	3.822	0.131	0.127
0.2	1.005	0.100	5.025	0.498	10.4	2.392	2.173	0.230	0.209	30.4	3.963	3.835	0.130	0.126
0.3	1.011	0.148	3.370	0.495	10.6	2.413	2.195	0.228	0.207	30.6	3.976	3.848	0.130	0.126
0.4	1.019	0.196	2.548	0.491	10.8	2.434	2.219	0.225	0.205	30.8	3.988	3.861	0.129	0.125
0.5	1.029	0.243	2.058	0.486	11.0	2.454	2.241	0.223	0.204	31.0	4.001	3.874	0.129	0.125
0.6	1.041	0.288	1.735	0.480	11.2	2.474	2.263	0.221	0.202	31.2	4.013	3.887	0.129	0.125
0.7	1.054	0.332	1.505	0.475	11.4	2.494	2.285	0.219	0.200	31.4	4.026	3.900	0.128	0.124
0.8	1.068	0.375	1.335	0.468	11.6	2.514	2.307	0.217	0.199	31.6	4.038	3.913	0.128	0.124
0.9	1.083	0.416	1.203	0.462	11.8	2.534	2.328	0.215	0.197	31.8	4.051	3.925	0.127	0.123
1.0	1.099	0.455	1.099	0.455	12.0	2.554	2.350	0.213	0.196	32.0	4.063	3.938	0.127	0.123
1.1	1.115	0.493	1.014	0.448	12.2	2.573	2.371	0.211	0.194	32.2	4.075	3.951	0.127	0.123
1.2	1.132	0.530	0.943	0.442	12.4	2.592	2.392	0.209	0.193	32.4	4.088	3.963	0.126	0.122
1.3	1.149	0.566	0.884	0.435	12.6	2.611	2.412	0.207	0.191	32.6	4.100	3.976	0.126	0.122
1.4	1.166	0.600	0.833	0.429	12.8	2.630	2.433	0.206	0.190	32.8	4.112	3.988	0.125	0.122
1.5	1.184	0.634	0.789	0.422	13.0	2.649	2.453	0.204	0.189	33.0	4.124	4.001	0.125	0.121
1.6	1.201	0.666	0.751	0.416	13.2	2.668	2.474	0.202	0.187	33.2	4.136	4.013	0.125	0.121
1.7	1.219	0.697	0.717	0.410	13.4	2.687	2.494	0.201	0.186	33.4	4.148	4.026	0.124	0.121
1.8	1.237	0.728	0.687	0.404	13.6	2.705	2.514	0.199	0.185	33.6	4.160	4.038	0.124	0.120
1.9	1.254	0.757	0.660	0.399	13.8	2.724	2.533	0.197	0.184	33.8	4.172	4.051	0.123	0.120
2.0	1.272	0.786	0.636	0.393	14.0	2.742	2.553	0.196	0.182	34.0	4.184	4.063	0.123	0.119
2.1	1.290	0.814	0.614	0.388	14.2	2.760	2.572	0.194	0.181	34.2	4.196	4.075	0.123	0.119
2.2	1.307	0.842	0.594	0.383	14.4	2.778	2.592	0.193	0.180	34.4	4.208	4.087	0.122	0.119
2.3	1.324	0.868	0.576	0.378	14.6	2.796	2.611	0.192	0.179	34.6	4.220	4.100	0.122	0.118
2.4	1.342	0.894	0.559	0.373	14.8	2.814	2.630	0.190	0.178	34.8	4.232	4.112	0.122	0.118
2.5	1.359	0.920	0.544	0.368	15.0	2.831	2.649	0.189	0.177	35.0	4.243	4.124	0.121	0.118
2.6	1.376	0.945	0.529	0.363	15.2	2.849	2.668	0.187	0.176	35.2	4.255	4.136	0.121	0.118
2.7	1.393	0.969	0.516	0.359	15.4	2.865	2.686	0.186	0.174	35.4	4.267	4.148	0.121	0.117
2.8	1.409	0.993	0.503	0.355	15.6	2.884	2.705	0.185	0.173	35.6	4.279	4.160	0.120	0.117
2.9	1.426	1.017	0.492	0.351	15.8	2.901	2.723	0.184	0.172	35.8	4.290	4.172	0.120	0.117
3.0	1.443	1.040	0.481	0.347	16.0	2.918	2.741	0.182	0.171	36.0	4.302	4.184	0.119	0.116
3.1	1.459	1.062	0.471	0.343	16.2	2.935	2.760	0.181	0.170	36.2	4.314	4.196	0.119	0.116
3.2	1.475	1.085	0.461	0.339	16.4	2.952	2.778	0.180	0.169	36.4	4.325	4.208	0.119	0.116
3.3	1.491	1.106	0.452	0.335	16.6	2.969	2.795	0.179	0.168	36.6	4.337	4.220	0.118	0.115
3.4	1.507	1.128	0.443	0.332	16.8	2.986	2.813	0.178	0.167	36.8	4.348	4.232	0.118	0.115
3.5	1.523	1.149	0.435	0.328	17.0	3.002	2.831	0.177	0.167	37.0	4.360	4.243	0.118	0.115
3.6	1.539	1.170	0.427	0.325	17.2	3.019	2.849	0.176	0.166	37.2	4.371	4.255	0.118	0.114
3.7	1.554	1.190	0.420	0.322	17.4	3.036	2.866	0.174	0.165	37.4	4.383	4.267	0.117	0.114
3.8	1.570	1.210	0.413	0.318	17.6	3.052	2.883	0.173	0.164	37.6	4.394	4.279	0.117	0.114
3.9	1.585	1.230	0.406	0.315	17.8	3.068	2.901	0.172	0.163	37.8	4.405	4.290	0.117	0.113
4.0	1.600	1.250	0.400	0.312	18.0	3.084	2.918	0.171	0.162	38.0	4.417	4.302	0.116	0.113
4.1	1.616	1.269	0.394	0.309	18.2	3.101	2.935	0.170	0.161	38.2	4.428	4.314	0.116	0.113
4.2	1.631	1.288	0.388	0.307	18.4	3.117	2.952	0.169	0.160	38.4	4.439	4.325	0.116	0.113
4.3	1.645	1.307	0.383	0.304	18.6	3.133	2.969	0.168	0.160	38.6	4.450	4.337	0.115	0.112
4.4	1.660	1.325	0.377	0.301	18.8	3.149	2.986	0.167	0.159	38.8	4.462	4.348	0.115	0.112
4.5	1.675	1.343	0.372	0.299	19.0	3.164	3.002	0.167	0.158	39.0	4.473	4.360	0.115	0.112
4.6	1.689	1.362	0.367	0.296	19.2	3.180	3.019	0.166	0.157	39.2	4.484	4.371	0.114	0.112
4.7	1.704	1.379	0.362	0.293	19.4	3.196	3.035	0.165	0.156	39.4	4.495	4.383	0.114	0.111
4.8	1.718	1.397	0.358	0.291	19.6	3.211	3.052	0.164	0.156	39.6	4.506	4.394	0.114	0.111
4.9	1.732	1.414	0.354	0.289	19.8	3.227	3.068	0.163	0.155	39.8	4.517	4.405	0.114	0.111
5.0	1.746	1.432	0.349	0.286	20.0	3.242	3.084	0.162	0.154	40.0	4.528	4.417	0.113	0.110
5.1	1.760	1.449	0.345	0.284	20.2	3.258	3.100	0.161	0.153	40.2	4.539	4.428	0.113	0.110
5.2	1.774	1.465	0.341	0.282	20.4	3.273	3.116	0.160	0.153	40.4	4.550	4.439	0.113	0.110
5.3	1.788	1.482	0.337	0.280	20.6	3.288	3.132	0.160	0.152	40.6	4.561	4.450	0.112	0.110
5.4	1.802	1.499	0.334	0.278	20.8	3.303	3.148	0.159	0.151	40.8	4.572	4.462	0.112	0.109
5.5	1.815	1.515	0.330	0.275	21.0	3.318	3.164	0.158	0.151	41.0	4.583	4.473	0.112	0.109
5.6	1.829	1.531	0.327	0.273	21.2	3.333	3.180	0.157	0.150	41.2	4.594	4.484	0.112	0.109
5.7	1.842	1.547	0.323	0.271	21.4	3.348	3.196	0.155	0.149	41.4	4.605	4.495	0.111	0.109
5.8	1.855	1.563	0.320	0.269	21.6	3.363	3.211	0.156	0.149	41.6	4.616	4.506	0.111	0.108
5.9	1.869	1.579	0.317	0.268	21.8	3.378	3.227	0.155	0.148	41.8	4.627	4.517	0.111	0.108
6.0	1.882	1.594	0.314	0.266	22.0	3.393	3.242	0.154	0.147	42.0	4.637	4.528	0.110	0.108
6.1	1.895	1.610	0.311	0.264	22.2	3.408	3.257	0.153	0.147	42.2	4.648	4.539	0.110	0.108
6.2	1.908	1.625	0.308	0.262	22.4	3.422	3.273	0.153	0.146	42.4	4.659	4.550	0.110	0.107
6.3	1.921	1.640	0.305	0.260	22.6	3.437	3.288	0.152	0.145	42.6	4.670	4.561	0.110	0.107
6.4	1.934	1.655	0.302	0.259	22.8	3.451	3.303	0.151	0.145	42.8	4.680	4.572	0.109	0.107
6.5	1.946	1.670	0.299	0.257	23.0	3.466	3.318	0.151	0.144	43.0	4.691	4.583	0.109	0.107
6.6	1.959	1.685	0.297	0.255	23.2	3.480	3.333	0.150	0.144	43.2	4.702	4.594	0.109	0.106
6.7	1.972	1.699	0.294	0.254	23.4	3.494	3.348	0.149	0.143	43.4	4.712	4.605	0.109	0.106
6.8	1.984	1.714	0.292	0.252	23.6	3.509	3.363	0.149	0.143	43.6	4.723	4.616	0.108	0.106
6.9	1.997	1.728	0.289	0.250	23.8	3.523	3.378	0.148	0.142	43.8	4.733	4.627	0.108	0.106
7.0	2.009	1.742	0.287	0.249	24.0	3.537	3.393	0.147	0.141	44.0	4.744	4.637	0.108	0.105
7.1	2.021	1.756	0.285	0.247	24.2	3.551	3.407	0.147	0.141	44.2	4.755	4.648	0.108	0.105
7.2	2.033	1.770	0.282	0.246	24.4	3.565	3.422	0.146	0.140	44.4	4.765	4.659	0.107	0.105
7.3	2.046	1.784	0.280	0.244	24.6	3.579	3.437	0.145	0.140	44.6	4.776	4.670	0.107	0.105
7.4	2.058	1.798	0.278	0.243	24.8	3.593	3.451	0.145	0.139	44.8	4.786	4.680	0.107	0.104
7.5	2.070	1.812	0.276	0.242	25.0	3.607	3.465	0.144	0.139	45.0	4.796	4.691	0.107	0.104
7.6	2.082	1.826	0.274	0.240	25.2	3.621	3.480	0.144	0.138	45.2	4.807	4.702	0.106	0.104
7.7	2.093	1.839	0.272	0.239	25.4	3.635	3.494	0.143	0.138	45.4	4.817	4.712	0.106	0.104
7.8	2.105	1.853	0.270	0.238	25.6	3.648	3.509	0.143	0.137	45.6	4.828	4.723	0.106	0.104
7.9	2.117	1.866	0.268	0.236	25.8	3.662	3.523	0.142	0.137	45.8	4.838	4.733	0.106	0.103
8.0	2.129	1.879	0.266	0.235	26.0	3.676	3.537	0.141	0.136	46.0	4.848	4.744	0.105	0.103
8.1	2.140	1.892	0.264	0.234	26.2	3.689	3.551	0.141	0.136	46.2	4.859	4.755	0.105	0.103
8.2	2.152	1.905	0.262	0.232	26.4	3.703	3.565	0.140	0.135	46.4	4.869	4.765	0.105	0.103
8.3	2.163	1.918	0.261	0.231	26.6	3.716	3.579	0.140	0.135	46.6	4.879	4.775	0.105	0.102
8.4	2.175	1.931	0.259	0.230	26.8	3.730	3.593	0.139	0.134	46.8	4.889	4.786	0.104	0.102
8.5	2.186	1.944	0.257	0.229	27.0	3.743	3.607	0.139	0.134	47.0	4.900	4.796	0.104	0.102
8.6	2.197	1.957	0.256	0.228	27.2	3.756	3.621	0.138	0.133	47.2	4.910	4.807	0.104	0.102
8.7	2.209	1.969	0.254	0.226	27.4	3.769	3.634	0.138	0.133	47.4	4.920	4.817	0.104	0.102
8.8	2.220	1.982	0.252	0.225	27.6	3.783	3.648	0.137	0.132	47.6	4.930	4.828	0.104	0.101
8.9	2.231	1.994	0.251	0.224	27.8	3.796	3.662	0.137	0.132	47.8	4.940	4.838	0.103	0.101
9.0	2.242	2.007	0.249	0.223	28.0	3.809	3.675	0.136	0.131	48.0	4.950	4.848	0.103	0.101
9.1	2.253	2.019	0.248	0.222	28.2	3.822	3.689	0.135	0.131	48.2	4.960	4.859	0.103	0.101
9.2	2.264	2.032	0.246	0.221	28.4	3.835	3.703	0.135	0.130	48.4	4.970	4.869	0.103	0.101
9.3	2.275	2.044	0.245	0.220	28.6	3.848	3.715	0.135	0.130	48.6	4.980	4.879	0.102	0.100
9.4	2.286	2.056	0.243	0.219	28.8	3.861	3.729	0.134	0.129	48.8	4.991	4.889	0.102	0.100
9.5	2.297	2.068	0.242	0.218	29.0	3.874	3.743	0.134	0.129	49.0	5.001	4.900	0.102	0.100
9.6	2.308	2.080	0.240	0.217	29.2	3.887	3.756	0.133	0.129	49.2	5.010	4.910	0.102	0.100
9.7	2.319	2.092	0.239	0.216	29.4	3.900	3.769	0.133	0.128	49.4	5.020	4.920	0.102	0.100
9.8	2.329	2.104	0.238	0.215	29.6	3.913	3.783	0.132	0.128	49.6	5.030	4.930	0.101	0.099
9.9	2.340	2.115	0.236	0.214	29.8	3.925	3.796	0.132	0.127	49.8	5.040	4.940	0.101	0.099

TABLE 1.1

TABLE OF F(P) AND G(P) FUNCTIONS

P	F(P)	G(P)	F(P)/P	G(P)/P	P	F(P)	G(P)	F(P)/P	G(P)/P	P	F(P)	G(P)	F(P)/P	G(P)/P
50.0	5.050	4.950	0.101	0.099	100.0	7.107	7.036	0.071	0.070	200.0	10.025	9.975	0.050	0.050
50.5	5.075	4.975	0.100	0.099	101.0	7.142	7.071	0.071	0.070	201.0	10.050	10.000	0.050	0.050
51.0	5.100	5.000	0.100	0.098	102.0	7.177	7.107	0.070	0.070	202.0	10.075	10.025	0.050	0.050
51.5	5.124	5.025	0.099	0.098	103.0	7.211	7.142	0.070	0.069	203.0	10.100	10.050	0.050	0.050
52.0	5.148	5.050	0.099	0.097	104.0	7.246	7.177	0.070	0.069	204.0	10.124	10.075	0.050	0.049
52.5	5.173	5.075	0.099	0.097	105.0	7.280	7.211	0.069	0.069	205.0	10.149	10.100	0.050	0.049
53.0	5.197	5.099	0.098	0.096	106.0	7.315	7.246	0.069	0.068	206.0	10.174	10.124	0.049	0.049
53.5	5.221	5.124	0.098	0.096	107.0	7.349	7.280	0.069	0.068	207.0	10.198	10.149	0.049	0.049
54.0	5.244	5.148	0.097	0.095	108.0	7.383	7.315	0.068	0.068	208.0	10.223	10.174	0.049	0.049
54.5	5.268	5.172	0.097	0.095	109.0	7.416	7.349	0.068	0.067	209.0	10.247	10.198	0.049	0.049
55.0	5.292	5.197	0.096	0.094	110.0	7.450	7.383	0.068	0.067	210.0	10.271	10.223	0.049	0.049
55.5	5.315	5.221	0.096	0.094	111.0	7.483	7.416	0.067	0.067	211.0	10.296	10.247	0.049	0.049
56.0	5.339	5.244	0.095	0.094	112.0	7.517	7.450	0.067	0.067	212.0	10.320	10.271	0.049	0.048
56.5	5.362	5.268	0.095	0.093	113.0	7.550	7.483	0.067	0.066	213.0	10.344	10.296	0.049	0.048
57.0	5.386	5.292	0.094	0.093	114.0	7.583	7.517	0.067	0.066	214.0	10.368	10.320	0.048	0.048
57.5	5.409	5.315	0.094	0.092	115.0	7.616	7.550	0.066	0.066	215.0	10.392	10.344	0.048	0.048
58.0	5.432	5.339	0.094	0.092	116.0	7.649	7.583	0.066	0.065	216.0	10.416	10.368	0.048	0.048
58.5	5.455	5.362	0.093	0.092	117.0	7.681	7.616	0.066	0.065	217.0	10.440	10.392	0.048	0.048
59.0	5.478	5.386	0.093	0.091	118.0	7.714	7.649	0.065	0.065	218.0	10.464	10.416	0.048	0.048
59.5	5.500	5.409	0.092	0.091	119.0	7.746	7.681	0.065	0.065	219.0	10.488	10.440	0.048	0.048
60.0	5.523	5.432	0.092	0.091	120.0	7.778	7.714	0.065	0.064	220.0	10.512	10.464	0.048	0.048
60.5	5.546	5.455	0.092	0.090	121.0	7.810	7.746	0.065	0.064	221.0	10.536	10.488	0.048	0.047
61.0	5.568	5.478	0.091	0.090	122.0	7.842	7.778	0.064	0.064	222.0	10.559	10.512	0.048	0.047
61.5	5.591	5.500	0.091	0.089	123.0	7.874	7.810	0.064	0.063	223.0	10.583	10.536	0.047	0.047
62.0	5.613	5.523	0.091	0.089	124.0	7.906	7.842	0.064	0.063	224.0	10.607	10.559	0.047	0.047
62.5	5.635	5.546	0.090	0.089	125.0	7.937	7.874	0.063	0.063	225.0	10.630	10.583	0.047	0.047
63.0	5.657	5.568	0.090	0.088	126.0	7.969	7.906	0.063	0.063	226.0	10.654	10.607	0.047	0.047
63.5	5.679	5.591	0.089	0.088	127.0	8.000	7.937	0.063	0.062	227.0	10.677	10.630	0.047	0.047
64.0	5.701	5.613	0.089	0.088	128.0	8.031	7.969	0.063	0.062	228.0	10.701	10.654	0.047	0.047
64.5	5.723	5.635	0.089	0.087	129.0	8.062	8.000	0.062	0.062	229.0	10.724	10.677	0.047	0.047
65.0	5.745	5.657	0.088	0.087	130.0	8.093	8.031	0.062	0.062	230.0	10.747	10.701	0.047	0.047
65.5	5.767	5.679	0.088	0.087	131.0	8.124	8.062	0.062	0.062	231.0	10.770	10.724	0.047	0.046
66.0	5.788	5.701	0.088	0.086	132.0	8.155	8.093	0.062	0.061	232.0	10.794	10.747	0.047	0.046
66.5	5.810	5.723	0.087	0.086	133.0	8.185	8.124	0.062	0.061	233.0	10.817	10.770	0.046	0.046
67.0	5.831	5.745	0.087	0.086	134.0	8.216	8.155	0.061	0.061	234.0	10.840	10.794	0.046	0.046
67.5	5.853	5.767	0.087	0.085	135.0	8.246	8.185	0.061	0.061	235.0	10.863	10.817	0.046	0.046
68.0	5.874	5.788	0.086	0.085	136.0	8.277	8.216	0.061	0.060	236.0	10.886	10.840	0.046	0.046
68.5	5.895	5.810	0.086	0.085	137.0	8.307	8.246	0.061	0.060	237.0	10.909	10.863	0.046	0.046
69.0	5.916	5.831	0.086	0.085	138.0	8.337	8.277	0.060	0.060	238.0	10.932	10.886	0.046	0.046
69.5	5.937	5.853	0.085	0.084	139.0	8.367	8.307	0.060	0.060	239.0	10.954	10.909	0.046	0.046
70.0	5.958	5.874	0.085	0.084	140.0	8.397	8.337	0.060	0.060	240.0	10.977	10.932	0.046	0.046
70.5	5.979	5.895	0.085	0.084	141.0	8.426	8.367	0.060	0.059	241.0	11.000	10.954	0.046	0.045
71.0	6.000	5.916	0.085	0.083	142.0	8.456	8.397	0.060	0.059	242.0	11.023	10.977	0.046	0.045
71.5	6.021	5.937	0.084	0.083	143.0	8.485	8.426	0.059	0.059	243.0	11.045	11.000	0.045	0.045
72.0	6.042	5.958	0.084	0.083	144.0	8.515	8.456	0.059	0.059	244.0	11.068	11.023	0.045	0.045
72.5	6.062	5.979	0.084	0.082	145.0	8.544	8.485	0.059	0.059	245.0	11.091	11.045	0.045	0.045
73.0	6.083	6.000	0.083	0.082	146.0	8.573	8.515	0.059	0.058	246.0	11.113	11.068	0.045	0.045
73.5	6.104	6.021	0.083	0.082	147.0	8.602	8.544	0.059	0.058	247.0	11.136	11.091	0.045	0.045
74.0	6.124	6.042	0.083	0.082	148.0	8.631	8.573	0.058	0.058	248.0	11.158	11.113	0.045	0.045
74.5	6.144	6.062	0.082	0.081	149.0	8.660	8.602	0.058	0.058	249.0	11.180	11.136	0.045	0.045
75.0	6.165	6.083	0.082	0.081	150.0	8.689	8.631	0.058	0.058	250.0	11.203	11.158	0.045	0.045
75.5	6.185	6.104	0.082	0.081	151.0	8.718	8.660	0.058	0.057	251.0	11.225	11.180	0.045	0.045
76.0	6.205	6.124	0.082	0.081	152.0	8.747	8.689	0.058	0.057	252.0	11.247	11.203	0.045	0.044
76.5	6.225	6.144	0.081	0.080	153.0	8.775	8.718	0.057	0.057	253.0	11.269	11.225	0.045	0.044
77.0	6.245	6.165	0.081	0.080	154.0	8.804	8.747	0.057	0.057	254.0	11.292	11.247	0.044	0.044
77.5	6.265	6.185	0.081	0.080	155.0	8.832	8.775	0.057	0.057	255.0	11.314	11.269	0.044	0.044
78.0	6.285	6.205	0.081	0.080	156.0	8.860	8.803	0.057	0.056	256.0	11.336	11.292	0.044	0.044
78.5	6.305	6.225	0.080	0.079	157.0	8.888	8.832	0.057	0.056	257.0	11.358	11.314	0.044	0.044
79.0	6.325	6.245	0.080	0.079	158.0	8.916	8.860	0.056	0.056	258.0	11.380	11.336	0.044	0.044
79.5	6.345	6.265	0.080	0.079	159.0	8.944	8.888	0.056	0.056	259.0	11.402	11.358	0.044	0.044
80.0	6.364	6.285	0.080	0.079	160.0	8.972	8.916	0.056	0.056	260.0	11.424	11.380	0.044	0.044
80.5	6.384	6.305	0.079	0.078	161.0	9.000	8.944	0.056	0.056	261.0	11.446	11.402	0.044	0.044
81.0	6.403	6.325	0.079	0.078	162.0	9.028	8.972	0.056	0.055	262.0	11.467	11.424	0.044	0.044
81.5	6.423	6.345	0.079	0.078	163.0	9.055	9.000	0.056	0.055	263.0	11.489	11.446	0.044	0.044
82.0	6.442	6.364	0.079	0.078	164.0	9.083	9.028	0.055	0.055	264.0	11.511	11.467	0.044	0.043
82.5	6.462	6.384	0.078	0.077	165.0	9.111	9.055	0.055	0.055	265.0	11.533	11.489	0.044	0.043
83.0	6.481	6.403	0.078	0.077	166.0	9.138	9.083	0.055	0.055	266.0	11.554	11.511	0.043	0.043
83.5	6.500	6.423	0.078	0.077	167.0	9.166	9.111	0.055	0.055	267.0	11.576	11.533	0.043	0.043
84.0	6.519	6.442	0.078	0.077	168.0	9.192	9.138	0.055	0.054	268.0	11.597	11.554	0.043	0.043
84.5	6.539	6.462	0.077	0.076	169.0	9.220	9.166	0.055	0.054	269.0	11.619	11.576	0.043	0.043
85.0	6.558	6.481	0.077	0.076	170.0	9.247	9.192	0.054	0.054	270.0	11.640	11.597	0.043	0.043
85.5	6.577	6.500	0.077	0.076	171.0	9.274	9.220	0.054	0.054	271.0	11.662	11.619	0.043	0.043
86.0	6.596	6.519	0.077	0.076	172.0	9.301	9.247	0.054	0.054	272.0	11.683	11.640	0.043	0.043
86.5	6.615	6.539	0.076	0.076	173.0	9.327	9.274	0.054	0.054	273.0	11.705	11.662	0.043	0.043
87.0	6.633	6.558	0.076	0.075	174.0	9.354	9.301	0.054	0.053	274.0	11.726	11.683	0.043	0.043
87.5	6.652	6.577	0.076	0.075	175.0	9.381	9.327	0.054	0.053	275.0	11.747	11.705	0.043	0.043
88.0	6.671	6.596	0.076	0.075	176.0	9.408	9.354	0.053	0.053	276.0	11.769	11.726	0.043	0.042
88.5	6.690	6.615	0.076	0.075	177.0	9.434	9.381	0.053	0.053	277.0	11.790	11.747	0.043	0.042
89.0	6.708	6.633	0.075	0.075	178.0	9.461	9.408	0.053	0.053	278.0	11.811	11.769	0.042	0.042
89.5	6.727	6.652	0.075	0.074	179.0	9.487	9.434	0.053	0.053	279.0	11.832	11.790	0.042	0.042
90.0	6.746	6.671	0.075	0.074	180.0	9.513	9.461	0.053	0.053	280.0	11.853	11.811	0.042	0.042
90.5	6.764	6.690	0.075	0.074	181.0	9.539	9.487	0.053	0.052	281.0	11.874	11.832	0.042	0.042
91.0	6.783	6.708	0.075	0.074	182.0	9.566	9.513	0.053	0.052	282.0	11.895	11.853	0.042	0.042
91.5	6.801	6.727	0.074	0.074	183.0	9.592	9.539	0.052	0.052	283.0	11.916	11.874	0.042	0.042
92.0	6.819	6.746	0.074	0.073	184.0	9.618	9.566	0.052	0.052	284.0	11.937	11.895	0.042	0.042
92.5	6.838	6.764	0.074	0.073	185.0	9.644	9.592	0.052	0.052	285.0	11.958	11.916	0.042	0.042
93.0	6.856	6.783	0.074	0.073	186.0	9.670	9.618	0.052	0.052	286.0	11.979	11.937	0.042	0.042
93.5	6.874	6.801	0.074	0.073	187.0	9.695	9.644	0.052	0.052	287.0	12.000	11.958	0.042	0.042
94.0	6.892	6.819	0.073	0.073	188.0	9.721	9.670	0.052	0.051	288.0	12.021	11.979	0.042	0.042
94.5	6.910	6.838	0.073	0.072	189.0	9.747	9.695	0.052	0.051	289.0	12.042	12.000	0.042	0.042
95.0	6.928	6.856	0.073	0.072	190.0	9.772	9.721	0.051	0.051	290.0	12.062	12.021	0.042	0.041
95.5	6.946	6.874	0.073	0.072	191.0	9.798	9.747	0.051	0.051	291.0	12.083	12.042	0.042	0.041
96.0	6.964	6.892	0.073	0.072	192.0	9.824	9.772	0.051	0.051	292.0	12.104	12.062	0.041	0.041
96.5	6.982	6.910	0.072	0.072	193.0	9.849	9.798	0.051	0.051	293.0	12.124	12.083	0.041	0.041
97.0	7.000	6.928	0.072	0.071	194.0	9.874	9.824	0.051	0.051	294.0	12.145	12.104	0.041	0.041
97.5	7.018	6.946	0.072	0.071	195.0	9.900	9.849	0.051	0.051	295.0	12.166	12.124	0.041	0.041
98.0	7.036	6.964	0.072	0.071	196.0	9.925	9.874	0.051	0.050	296.0	12.186	12.145	0.041	0.041
98.5	7.054	6.982	0.072	0.071	197.0	9.950	9.900	0.051	0.050	297.0	12.207	12.166	0.041	0.041
99.0	7.071	7.000	0.071	0.071	198.0	9.975	9.925	0.050	0.050	298.0	12.227	12.186	0.041	0.041
99.5	7.089	7.018	0.071	0.071	199.0	10.000	9.950	0.050	0.050	299.0	12.247	12.207	0.041	0.041

2. Characteristics of Cylindrical Dipoles and Monopoles

a. THE APPARENT ADMITTANCE

The cylindrical dipole consists of a highly-conducting tube or rod with radius a and half-length h. In practice, it is center-driven from a balanced open-wire transmission line with a distance b between the axes of the identical conductors of the line as shown in Fig. 2.1a. The cylindrical monopole is essentially half a dipole. It consists of a highly-conducting tube or rod with radius a and length h, erected perpendicular to a sufficiently large (ideally infinite), highly-conducting ground plane in either of the arrangements shown in Figs. 2.1b and 2.1c. The axis of the single wire with radius a in Fig. 2.1b is at a distance $b/2$ from the ground plane; with its image in the highly-conducting plane it is equivalent to the open line in Fig. 2.1a. The inner radius of the outer conductor of the coaxial line in Fig. 2.1c is b; the radius of the inner conductor is a and its extension of length h above the ground plane is the monopole antenna. In order that radiation from a balanced open-wire line be negligible, the condition

$$k_0 b = \frac{2\pi b}{\lambda} \ll 1 \tag{2.1}$$

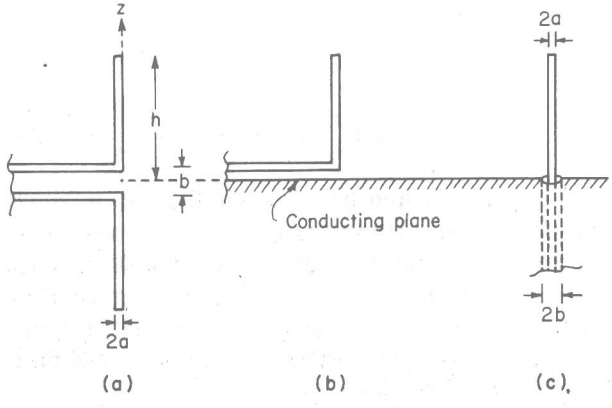

Fig. 2.1. Cylindrical antennas driven from open-wire and coaxial lines.

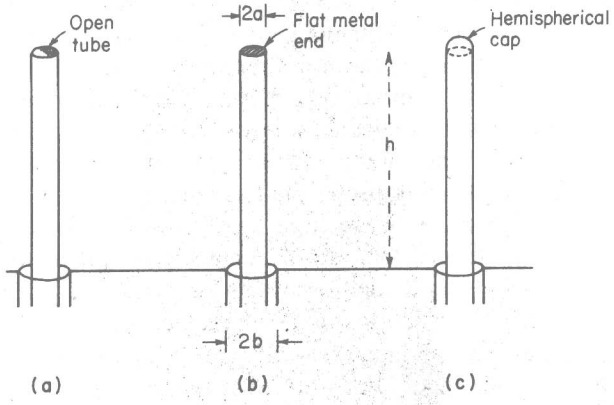

Fig. 2.2. Cylindrical monopoles with open, closed flat, and closed hemispherical ends.

must be satisfied. Similarly, in order to ensure that only the TEM mode can propagate in the coaxial line, the conditions

$$k_0 b < 1, \quad k_0(b-a) < 1 \tag{2.2}$$

must be fulfilled. Of these, the first condition is required to exclude TE modes, the second, less severe condition, to exclude TM modes. If complete rotational symmetry is maintained in the entire generating–transmitting–radiating system, TE modes may be absent because they are nowhere generated. In this case, only the second condition in (2.2) is required.

The end (ends) of the monopole (dipole) may be open as in Fig. 2.2a, consist of a flat metal disk as in Fig. 2.2b, or be capped with a metal hemisphere as in Fig. 2.2c. In the case of the open tube or the rod with a flat metal end, the axial length (half-length) is h; with a hemispherical cap it is $h' = h + a$.

From the point of view of a generator supplying power at the input end of a transmission line, a cylindrical dipole or monopole terminating the other end of the line behaves like any other load in the sense that it is observed as an apparent admittance $Y_a = G_a + jB_a$. It can be determined experimentally by means

of well-known techniques of measurement of the standing-wave pattern along the line.[1] Since conventional transmission-line theory, upon which most high-frequency measurements depend, is not accurate at and near the ends of the line,[2] the quantity actually measured is the admittance looking toward the load at a cross section of the line that is a half wavelength from the end. Owing to end effects on the transmission line and coupling between the antenna and the line over distances from their junction that are comparable with the line spacing (b for open wires, $b - a$ for coaxial lines), the apparent admittance Y_a depends on the physical properties of the junction region as well as on those of the antenna proper. It follows that the smaller b or $b - a$, the more nearly Y_a approaches a quantity characteristic exclusively of the antenna. Owing to the complicated nonrotationally symmetric properties of the antenna driven by an open-wire line, no mathematically useful limit is reached as $b \to 2a$. On the other hand, the limit $(b - a) \to 0$ for the coaxial line defines a physically unavailable but mathematically useful delta-function generator, which maintains at $z = 0$ a finite voltage across a "zero" gap that corresponds physically to an infinite knife-edge capacitance. The admittance seen by the emf of such a generator involves no transmission line but does include, in addition to the cylindrical surface of the antenna proper, the circular knife edges. Hence, the susceptance is infinite. However, for electrically thin antennas, the charging current associated with the infinite susceptance of these knife edges is highly localized in a narrow region very near the driving point and can be separated from the current associated with the cylindrical surface.[3,4] This process of "subtracting out" the current that charges the knife-edge capacitance is necessarily arbitrary and approximate. However, the various theoretical and experimental procedures that have been suggested are in good agreement with one another and the resulting finite susceptance is useful in determining the measurable apparent admittance of antennas driven from actual transmission lines in conjunction with lumped terminal-zone networks appropriate to the geometries of different lines.[5–7]. Only in certain special cases are terminal-zone effects sufficiently small to make the uncorrected ideal admittance a good approximation.[8]

b. THE MONOPOLE DRIVEN FROM A COAXIAL LINE

Owing to the complicated geometry of the junction region between the antenna and the transmission line, analytically accurate formulas for the apparent admittance of an antenna as a termination for the line are generally unavailable. An exception is the monopole driven from a coaxial line in the arrangement shown in Fig. 2.1c. For this rotationally symmetric configuration the apparent admittance has been determined for an infinitely long monopole subject to the following conditions:

$$(b - a)/a \ll 1, \qquad k_0(b - a) \ll 1 \tag{2.3}$$

[The severer condition ($k_0 b \ll 1$) need not be imposed if TE modes are nowhere generated.] The rigorous formula is[9]

$$Y_{a\infty}(k_0 a, b/a) = \frac{2\pi}{\zeta_0}\{F_{1\infty}(k_0 a) + jk_0 a F_{2\infty}(b/a)\} \tag{2.4}$$

where

$$F_{1\infty}(k_0 a) = \frac{2jka}{\pi}\left[1 - \ln\frac{4}{\pi} - \ln\frac{k_0 a}{2} - \gamma - C_0(k_0 a)\right] \tag{2.5a}$$

$$F_{2\infty}(b/a) = -\frac{2}{\pi}\ln(b/a - 1) \tag{2.5b}$$

and

$$C_0(k_0 a) = \int_0^\infty \left[\frac{H_1^{(1)}(\xi a)}{H_0^{(1)}(\xi a)} - j\right]\frac{dx}{\xi} + j\frac{\pi}{2} \tag{2.5c}$$

In these formulas $\xi = \sqrt{k_0^2 - x^2}$ and $\gamma = 0.577\ldots$. Note that $F_{1\infty}(k_0 a)$ is a complex function of $k_0 a$ and is independent of b/a, whereas $F_{2\infty}(b/a)$ is a real function of b/a alone.

The apparent admittance has also been evaluated[9] under the simplifying assumption that there are no end effects on the coaxial line, so that only the TEM mode exists at its end. The admittance $Y_{a\,\mathrm{TEM}}$ in this case is given by

$$Y_{a\infty} - Y_{a\mathrm{TEM}} = j(B_{a\infty} - B_{a\mathrm{TEM}}) = -j\frac{4k_0 a}{\zeta_0}\ln\frac{4}{\pi}$$

$$= -j16.1\frac{a}{\lambda}\ \text{millimhos} \tag{2.6}$$

So far the discussion has been confined to infinitely long monopoles. However, since both transmission-line end effects and the coupling between the antenna and the coaxial line are limited to short distances from the junction of the monopole with the line, a formula like (2.4) must also be true for monopoles of finite length h provided that

$$(b - a)/h \ll 1 \tag{2.7}$$

That is,

$$Y_a(k_0h, k_0a, b/a) = \frac{2\pi}{\zeta_0}[F_1(k_0h, k_0a) + jk_0aF_2(k_0h, b/a)] \quad (2.8)$$

where $F_1(k_0h, k_0a)$ is a complex function of k_0h and k_0a that is independent of b/a, and $F_2(k_0h, b/a)$ is a real function of k_0h and b/a that is independent of k_0a. Since $F_2(k_0h, b/a)$ is real, the real and imaginary parts of $Y_a = G_a + jB_a$ are expressed as follows:

$$G_a(k_0h, k_0a) = \frac{2\pi}{\zeta_0}\operatorname{Re} F_1(k_0h, k_0a) \quad (2.9a)$$

$$B_a(k_0h, k_0a, b/a) = \frac{2\pi}{\zeta_0}[\operatorname{Im} F_1(k_0h, k_0a) + k_0aF_2(k_0h, b/a)] \quad (2.9b)$$

where Re and Im stand for the real and imaginary parts. Note that the apparent conductance $G_a(k_0h, k_0a)$ is independent of b/a, whereas the apparent susceptance $B_a(k_0h, k_0a, b/a)$ is not.

It is readily shown that the following relation is valid:[10]

$$B_a(k_0h, k_0a, b/a) = B_a[k_0h, k_0a, (b/a)_2] + [k_0a/(k_0a)_1]\{B_a[k_0h, (k_0a)_1, b/a] - B_a[k_0h, (k_0a)_1, (b/a)_2]\} \quad (2.10)$$

This formula is conveniently used to determine nm values of $B_a(k_0h, k_0a, b/a)$ from n known values of $B_a[k_0h, (k_0a)_i, (b/a)_2]$, $i = 1, 2, \ldots, n$, and m known values of $B_a[k_0h, (k_0a)_1, (b/a)_p]$, $p = 1, 2, \ldots, m$. Note that $(k_0a)_1$ and $(b/a)_2$ are arbitrarily selected values in the range $(k_0a)_i$, $i = 1, 2, \ldots, n$, and $(b/a)_p$, $p = 1, 2, \ldots, m$. The practical significance of (2.10) is that with it the tabulation of the $n + m$ values, $B_a[k_0h, (k_0a)_1, (b/a)_p]$, $p = 1, 2, \ldots, m$, and $B_a[k_0h, (k_0a)_i, (b/a)_2]$, $i = 1, 2, \ldots, n$, is sufficient to make available all of the nm values, $B_a[k_0h, (k_0a)_i, (b/a)_p]$, $i = 1, 2, \ldots, n$; $p = 1, 2, \ldots, m$.

The formulas (2.8)–(2.10) are valid for the exact apparent admittance $Y_a = G_a + jB_a$ and for the approximate values obtained if only the TEM mode is assumed to exist in the coaxial feed line at its junction with the antenna. When (2.3) is satisfied, a formula like (2.6) is valid for antennas of finite length. Specifically,

$$G_a(k_0h, k_0a) = G_{a\text{TEM}}(k_0h, k_0a) \quad (2.11a)$$

$$B_a(k_0h, k_0a, b/a) = B_{a\text{TEM}}(k_0h, k_0a, b/a) - j16.1\frac{a}{\lambda}\text{ millimhos} \quad (2.11b)$$

From these the exact values are readily obtained from the tabulated approximate TEM values in Table 2.1. A sample graph of the admittance in the complex plane is shown in Fig. 2.3. The theoretical points obtained from Table 2.1 are shown. From this graph the extreme values of G and B are readily obtained as well as values intermediate to those computed. Note that large parts of the curve are sections of circles so that only three or four points are needed to determine a wide range of values.

Distributions of current along tubular monopoles with selected lengths are given in Table 2.2. The admittances of hemispherically capped monopoles with axial lengths $h + a$ are given in Table 2.3. Owing to approximations in treating the hemispherical cap, these are somewhat less accurate than the corresponding values for the open tube in Table 2.1.

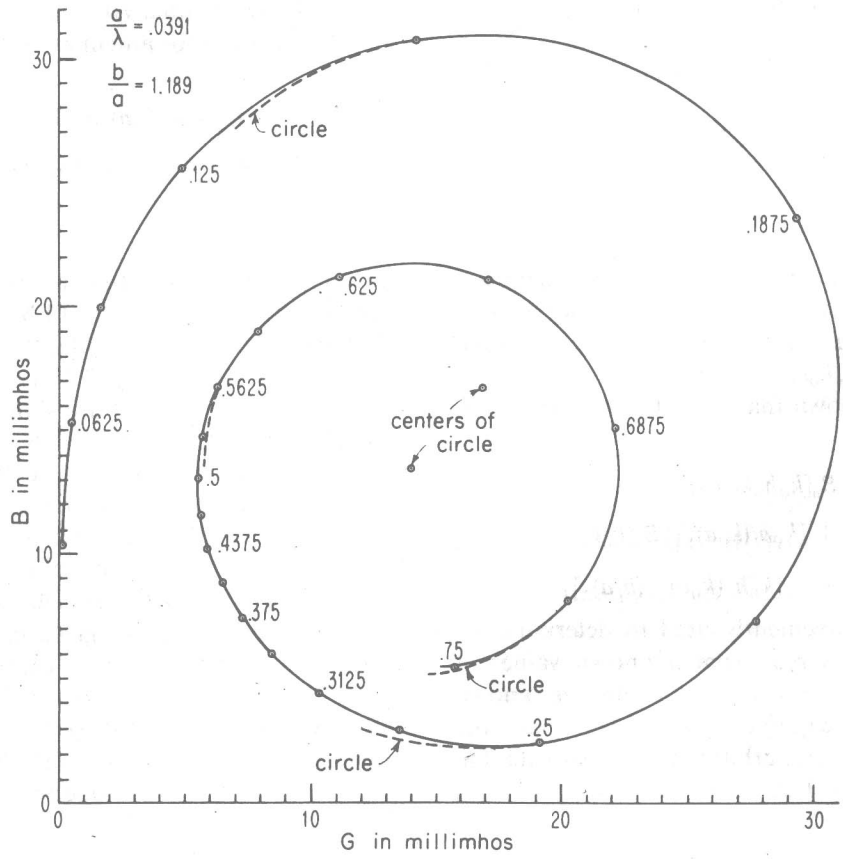

Fig. 2.3. Admittance of the tubular monopole.

TABLE 2.1

ADMITTANCE OF THE TUBULAR MONOPOLE

DIMENSIONS OF THE FEEDING COAXIAL LINE: b/a = 1.189

Y = G + jB (millimhos)

		a/λ (k_0a)				
h/λ	k_0h	.0064 (.0402)	.0127 (.0798)	.0190 (.1194)	.0254 (.1596)	.0318 (.1998)
.03125	0.196	0.00 + j3.14	0.01 + j4.87	0.02 + j6.43	0.04 + j7.89	0.06 + j9.22
.06250	0.393	0.03 + j4.86	0.07 + j7.23	0.14 + j9.36	0.22 + j11.38	0.33 + j13.28
.09375	0.589	0.14 + j6.65	0.30 + j9.63	0.51 + j12.32	0.79 + j14.87	1.13 + j17.28
.12500	0.785	0.49 + j9.00	1.02 + j12.81	1.70 + j16.22	2.56 + j19.42	3.57 + j22.39
.15625	0.982	1.76 + j12.68	3.59 + j17.68	5.82 + j21.84	8.40 + j25.35	11.13 + j28.18
.18750	1.178	7.47 + j18.88	13.92 + j23.29	19.60 + j24.81	23.95 + j24.79	26.97 + j24.18
.21875	1.374	27.60 + j12.61	29.30 + j7.66	28.85 + j6.00	28.30 + j5.81	27.95 + j6.29
.25000	1.571	17.24 - j7.12	17.21 - j4.85	17.49 - j2.86	17.92 - j1.03	18.43 + j0.64
.28125	1.767	8.24 - j5.62	9.65 - j3.70	10.72 - j1.94	11.67 - j0.29	12.55 + j1.24
.31250	1.963	5.10 - j3.21	6.47 - j1.61	7.47 - j0.06	8.51 + j1.43	9.40 + j2.84
.34375	2.160	3.70 - j1.46	4.89 + j0.08	5.86 + j1.59	6.75 + j3.05	7.57 + j4.43
.37500	2.356	2.95 + j0.16	3.99 + j1.45	4.87 + j2.99	5.68 + j4.47	6.43 + j5.87
.40625	2.552	2.49 + j0.89	3.43 + j2.60	4.23 + j4.21	4.98 + j5.75	5.69 + j7.21
.43750	2.749	2.20 + j1.80	3.07 + j3.64	3.81 + j5.35	4.52 + j6.96	5.19 + j8.49
.46875	2.945	2.01 + j2.65	2.82 + j4.64	3.54 + j6.45	4.22 + j8.17	4.89 + j9.78
.50000	3.142	1.89 + j3.50	2.69 + j5.65	3.40 + j7.60	4.09 + j9.44	4.76 + j11.15
.53125	3.338	1.84 + j4.41	2.66 + j6.76	3.40 + j8.88	4.13 + j10.85	4.86 + j12.70
.56250	3.534	1.89 + j5.45	2.79 + j8.06	3.63 + j10.38	4.47 + j12.52	5.33 + j14.52
.59375	3.731	2.12 + j6.76	3.22 + j9.70	4.29 + j12.25	5.40 + j14.59	6.53 + j16.71
.62500	3.927	2.76 + j8.55	4.37 + j11.87	5.98 + j14.63	7.64 + j17.04	9.30 + j19.10
.65625	4.123	4.58 + j11.10	7.45 + j14.55	10.17 + j16.98	12.69 + j18.73	14.92 + j19.98
.68750	4.320	10.24 + j13.64	14.98 + j14.85	18.00 + j14.93	19.90 + j14.82	21.13 + j14.84
.71875	4.516	19.60 + j6.41	20.07 + j4.95	19.98 + j5.06	19.94 + j5.78	20.00 + j6.76
.75000	4.712	13.74 - j3.63	13.86 - j1.56	14.18 + j0.31	14.61 + j2.05	15.10 + j3.68